

# Calculation of the Fermi Surface with Complex Topology from Norm-Conserving Cluster Perturbation Theory for Doping Dependent Electronic Structure of the Hubbard Model<sup>†</sup>

S. G. Ovchinnikov<sup>a,b</sup> and S. V. Nikolaev<sup>c</sup>

<sup>a</sup> Kirensky Institute of Physics, Siberian Branch, Russian Academy of Sciences, Krasnoyarsk, 660036 Russia

<sup>b</sup> Siberian Federal University, Krasnoyarsk, 660041 Russia

<sup>c</sup> Omsk State University, Omsk, 644077 Russia

e-mail: sgo@iph.krasn.ru

Received February 24, 2011; in final form, March 18, 2011

The results of recently developed norm-conserving cluster perturbation theory for doping dependent electronic structure of the Hubbard model are reported. We have found that the momentum distribution of the spectral weight strongly depends on the broadening value  $\delta$ . At  $\delta = 0.1t$ , we reproduce the angle-resolved photoemission spectroscopy data, while at  $\delta = 0.01t$  we obtain two quantum phase transitions.

DOI: 10.1134/S0021364011090116

Angle-resolved photoemission spectroscopy (ARPES) provides a lot of valuable experimental data on the electronic structure of cuprates [1]. It was found that Fermi surface has the form of arc around nodal point  $(\pi/2, \pi/2)$  with the pseudogap around antinodal points  $(\pi, 0)$  and  $(0, \pi)$  in the underdoped region. In the overdoped region, ARPES has found the large Fermi surface around  $(\pi, \pi)$ . The doping of an antiferromagnetic insulator results in a small hole pocket around nodal point which was observed by quantum oscillations measurements [2]. One side of the pocket is the Fermi arc (see discussion of ARPES and oscillations data in the recent review [3]). There is no smooth transformation of the Fermi surface from underdoped to overdoped region; it requires two quantum phase transitions [4]. Nevertheless, there are no ARPES indications for such transitions. Here we report the results of recently developed norm-conserving (NC) cluster perturbation theory (CPT) [5] for doping dependent electronic structure of the Hubbard model. We have found that the momentum distribution of the spectral weight  $A(\mathbf{k}, \epsilon_F)$  strongly depends on the broadening value  $\delta$ . At  $\delta = 0.1$  (in units of nearest neighbor hopping  $t$ ) we reproduce the ARPES data, while at  $\delta = 0.01$  we obtain two quantum phase transitions.

The most evident effect of strong electron correlations is the “no-double occupancy” constraint that is universal for any system with strong electron correlations. Specific for cuprates with their quasi-2D mag-

netic structure is the importance of the spatial spin correlations (short-range magnetic order) induced by large intraplane exchange interaction  $J = 2t^2/U$  ( $U$  is the Hubbard intra-atomic Coulomb parameter). The neglection of the spatial corrections makes the dynamical mean field theory (DMFT) inapplicable for cuprates. Taking into account both “no-double occupancy” constraint and short-range magnetic order several groups have found the intermediate regime in Fermi surface topology between small pockets in underdoped and large pocket in overdoped [6–10]. Different cluster extensions of DMFT [11–15] have also found the importance of the short-range spin correlations for the formation the pseudogap around the antinodal point in hole-doped cuprates. Using the most advanced cellular DMFT plus exact diagonalization (CDFT + ED) method [11] the three type of the Fermi surfaces have been obtained [13] exactly the same as in papers [6–10]. Thus different theoretical approaches result in the existence of the intermediate region in the hole concentration scale  $p$  at  $p_{c1} < p < p_{c2}$ . At  $p < p_{c1}$  there are small hole pockets, while at  $p > p_{c2}$  the large Fermi surface corresponds to the conventional band theory. The critical values  $p_{c1}$  and  $p_{c2}$  depend on the model parameters and approximation made. The ab initio calculated parameters of the  $t-t'-J$  model result in  $p_{c1} = 0.15$  and  $p_{c2} = 0.247$ .

In the intermediate region the Fermi surface is formed by hole and electron sheets around  $(\pi, \pi)$  with electron one collapsed at  $p \rightarrow p_{c2}$  [4, 7]. Up to now there is no experimental evidence for such Fermi surface from ARPES and quantum oscillations measure-

<sup>†</sup>The article is published in the original.

ments. All quantum oscillations studies are restricted to the underdoped region, presumably due to sample quality [3]. To analyze why ARPES does not see the intermediate Fermi surface we have studied here the hole dispersion and spectral weight  $A(\mathbf{k}, \varepsilon_F)$  by the NC-CPT method that was used to study undoped Hubbard model recently [5].

Cluster models can be formulated in a general functional framework [16–18]. In the initial version [19] the CPT consists of (i) dividing the lattice into identical  $N$ -site clusters, (ii) evaluating—by exact diagonalization—the one-particle Green's function  $G_0(\omega)$  for cluster with open boundary conditions, and (iii) treating the intercluster hopping  $t$  in perturbation theory and recovering the crystal Green's function  $G(\mathbf{k}, \omega)$ . Thus, short-range effects are treated exactly, while long-distance propagation is treated at the single-particle analog.

Usually step (ii) proceeds according to the Lanczos method. In  $2 \times 2$  cluster for the Hubbard model the number of eigenstates is equal to  $4^4 = 256$ . The Lanczos method takes into account only the ground and a few excited states ignoring all other. If we write down the exact representation of the electron creation operator at atom  $f$  with spin projection  $\sigma$  in terms of the multielectron eigenstates  $|p\rangle$  and  $|q\rangle$  of the cluster

$$a_{f\sigma}^\dagger = \sum_{p,q=1}^{256} \langle p | a_{f\sigma}^\dagger | q \rangle |p\rangle\langle q|, \quad (1)$$

then the Fermi anticommutator

$$\{a_{f\sigma}, a_{f\sigma}^\dagger\}_+ = 1 \quad (2)$$

can be treated as the sum rule providing the norm conservation for electron. We want to emphasize that this sum rule is satisfied only when all cluster eigenstates are included in the right side of the Eq. (1). Ignoring excited states results in the violation of the sum rule. In another words some part of electron spectral weight will be lost. Let us introduce the  $f$ -factor to measure total spectral weight

$$f = \int d\omega A(\mathbf{k}, \omega). \quad (3)$$

The exact value for  $f = 1$  is achieved only when all excited eigenstates are included. Contrary, if one restrict himself only to the lowest in energy multielectron states with  $|n_e = 4, S = 0\rangle$  and  $|n_e = 3, S = 1/2\rangle$ ,  $|n_e = 5, S = 1/2\rangle$  (basis for “effective single band Hubbard model”) the  $f$ -factor is equal to  $f = 0.395$ . As was shown in recent work [5] it is possible to get  $f \approx 0.999$  by taking into account 15–20 excited states. The calculation with controlled  $f$ -factor with  $1 - f$  less than 1% we call the norm conserving one.

The Hubbard operators  $X_i^{pq} = |p\rangle\langle q|$  for the cluster centered at  $\mathbf{R}_i$  naturally appear in the right side of Eq. (1). In this representation electron is given by a

linear combination of the Hubbard fermions (excitations between  $|N_e, S\rangle$  and  $|N_e \pm 1, S \pm 1/2\rangle$  configurations). It is convenient to introduce a vector  $\alpha = (p, q)$  instead of a pair of final  $p$  and initial  $q$  states [20]. Each vector  $\alpha$  corresponds to some Hubbard fermion if  $\gamma_\sigma(\alpha) = \langle p | a_{f\sigma}^\dagger | q \rangle \neq 0$ . The main CPT equation [19] for the Fourier transform of the lattice Green's function  $D_{\alpha\beta} = \langle\langle X_f^\alpha | X_g^\beta \rangle\rangle$  is just a Hubbard-I approximation for the intercluster hopping  $T(\mathbf{k})$ :

$$D^{-1}(\mathbf{k}, \omega) = (D^0(\omega))^{-1} - T(\mathbf{k}). \quad (4)$$

Here all functions are matrices in  $\alpha, \beta$  index, and

$$D_{\alpha\beta}^0(\omega) = \delta_{\alpha\beta} F(\alpha)/[\omega - \Omega(\alpha)], \quad (5)$$

$$\Omega(\alpha) = E_q(N+1) - E_p(N) - \mu, \quad (6)$$

$$F(\alpha) = \langle X^{pp} \rangle + \langle X^{qq} \rangle. \quad (7)$$

Here  $D_{\alpha\beta}^0(\omega)$  is the exact cluster Green's function. Its spectral weight may be zero when it describes the excitation between two empty states. Similar to the CDMFT + ED calculations [11, 13] our NC-CPT, as shown below in the Fig. 1, reproduces both poles and zeros of the electronic Green's function

$$G_{\sigma\sigma'}(\mathbf{k}, \omega) = \frac{1}{N_c} \sum_{i,j=1}^{N_c} \sum_{\alpha\beta} \gamma_{i\sigma}(\alpha) \gamma_{j\sigma'}^*(\beta) \times D_{\alpha\beta}(\mathbf{k}, \omega) e^{-i(\mathbf{r}_i - \mathbf{r}_j)\mathbf{k}}, \quad (8)$$

where  $N_c$  is the number of sites in the cluster (4 in our case);  $i, j$  are site indexes in the cluster.

Doping results the redistribution of the spectral weight and change the band structure. For three different concentrations we plot in Fig. 1 the poles and zeros (left column) and map of the spectral weight  $A(\mathbf{k}, \varepsilon_F)$  (momentum distribution curves or MDC in ARPES). The spectral weight

$$A(\mathbf{k}, \omega) = -\frac{1}{\pi} \text{Im} G(\mathbf{k}, \omega + i\delta) \quad (9)$$

depends on the broadening  $\delta$ . The central and right columns in Fig. 1 correspond to the different values of  $\delta$ . The model parameters are

$$U/t = 4.3, \quad t'/t = -0.13, \quad t''/t = 0.16,$$

$$\delta/t = 0.01 \quad (\text{Figs. 1b, 1e, 1h}),$$

$$\delta/t = 0.1 \quad (\text{Figs. 1c, 1f, 1i}).$$

The energy windows around Fermi level for spectral weight map was  $\pm 0.2t$  for  $\delta/t = 0.1$  and  $\pm 0.02t$  for  $\delta/t = 0.01$ .

The tight-binding fitting reproduce the ARPES data for optimal doping rather well (for example, for LSCO and Bi-2212). The nearest neighbor hopping integral found by this fitting  $t \approx 0.25\text{--}0.4$  eV [21–23].

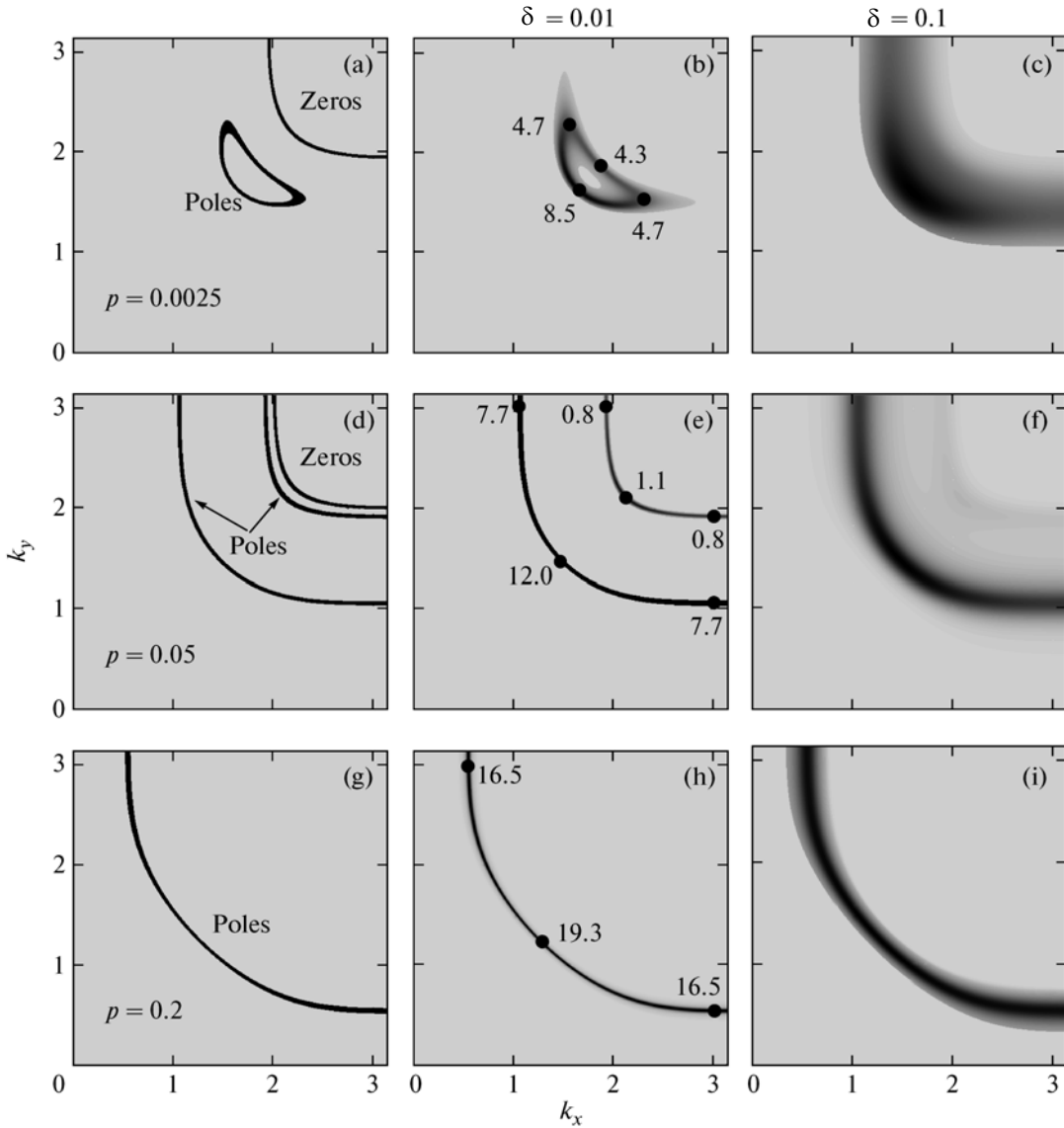


**Fig. 1.** Fermi surface in three different concentration regions: from poles and zeros of the Green-function (a) and spectral weight map with high resolution (b) and low resolution (c) for doping value  $p = 0.0025$ . The same in (d, e, f) for  $p = 0.05$  and (g, h, i) for  $p = 0.20$ . The numbers at the different  $k$  points in (b, e, h) show the spectral weight in this point.

During last 10–15 years the typical energy resolution for ARPES was 10–45 meV [23–26]. Therefore, authors of many theoretical works take the broadening parameter to be 0.02–0.15 $t$  [12–15]. For instance, Fermi arc has been measured by ARPES in LSCO [23] with resolution  $\delta = 0.02$  eV. The value of hopping parameter fitted the Fermi surface in that paper is  $t = 0.25$  eV, thus we estimate the ratio  $\delta/t = 0.08$ . However, in the present days there is the laser-excited ARPES with the energy resolution about 1 meV [27].

At small doping the Fermi surface shows a small pocket (Fig. 1a). In the limit of small broadening the MDC gives also the same pocket. We have calculated it with different  $\delta = 0.01t$  and  $\delta = 0.1t$  (Figs. 1b, 1c).

Nevertheless, the spectral weight varies along the pocket decreasing close to the line of zeros similar to the paper [11]. The resolution value  $\delta = 0.1t$  results a transformation of the pocket into the arc (Fig. 1c) (similar transformation is obtained in the paper [13] for  $\delta = 0.05t$ ). This transformation has been discussed by many authors before as mentioned in the review [3]. In the intermediate region  $p_{c1} < p < p_{c2}$  the two Fermi surface and line of zeros around  $(\pi, \pi)$  are shown in Fig. 1d. The MDC reveals for small  $\delta$  in Fig. 1e that the larger hole surface has also the order of magnitude large spectral weight than small electron surface. The MDC for  $\delta = 0.1t$  (Fig. 1f) shows only one large hole Fermi surface while electron surface disappeared. Its spectral weight becomes too small.

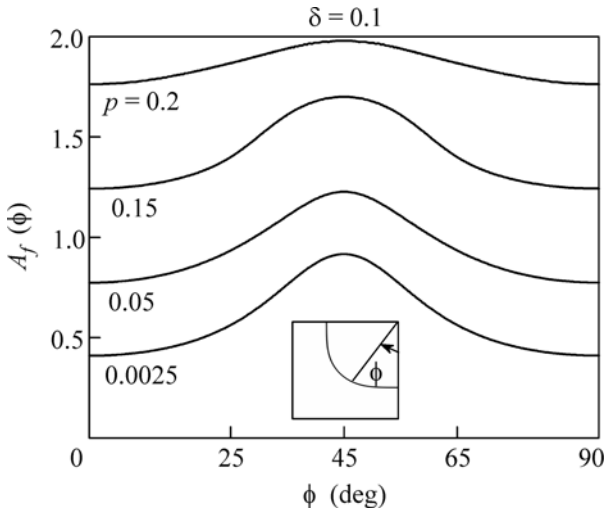


**Fig. 2.** Angle dependence of the spectral weight along the Fermi surface for different doping values and broadening  $\delta = 0.1t$ .

Finally at large doping both the poles (Fig. 1g) and MDC (Figs. 1h, 1i) show the same Fermi surface independently of the broadening value.

The concentration dependence of the spectral weight for  $\delta = 0.1t$  is shown in Fig. 2. The suppression of the spectral weight in the antinodal point related to the pseudogap is maximal at small doping and gradually decreases with increasing doping. This behavior corresponds well to the ARPES data [1].

In conclusion, we have shown that the concentration dependence of the true Fermi surface (left column in Fig. 1) and MDC with low resolution (right column in Fig. 1) gives different results. While the Fermi surface has three different types of topology separated by two Lifshitz transitions the ARPES gives the arc with smoothly increasing length. Only order of magnitude improvement in energy resolution will allow one to obtain the true Fermi surface by MDC as shown in the central column in Fig. 1.

This work was supported by the Presidium of the Russian Academy of Sciences (program no. 18.7); the Russian Foundation for Basic Research (project nos. 09-02-00127, 10-02-90725-mob\_st); Siberian Branch, Russian Academy of Sciences (Integration Project no. N40); and the Ministry of Education and Sciences of the Russian Federation (state contract no. P891, Program “Kadry”).

## REFERENCES

1. A. Damascelli, Z. Hussain, and Z. X. Shen, Rev. Mod. Phys. **75**, 473 (2003).
2. N. Doiron-Leyraud, C. Proust, D. LeBoeuf, et al., Nature **447**, 565 (2007).
3. M. R. Norman, Physics **3**, 86 (2010).
4. S. G. Ovchinnikov, E. I. Shneyder, and M. M. Korshunov, J. Phys.: Condens Matter **23**, 045701 (2011).
5. S. V. Nikolaev and S. G. Ovchinnikov, J. Exp. Theor. Phys. **111**, 634 (2010).
6. A. F. Barabanov, A. A. Kovalev, O. V. Urazaev, et al., J. Exp. Theor. Phys. **92**, 677 (2001).
7. S. G. Ovchinnikov and M. M. Korshunov, Eur. Phys. J. B **57**, 271 (2007).
8. N. M. Plakida and V. S. Oudovenko, J. Exp. Theor. Phys. **104**, 230 (2007).
9. L. Hosoi, M. S. Laad, and P. Fulde, Phys. Rev. B **78**, 165107 (2008).
10. S. Chakravarty and H.-Y. Kee, Proc. Natl. Acad. Sci. (USA) **105**, 8835 (2008).
11. T. D. Stanescu and G. Kotliar, Phys. Rev. B **74**, 125110 (2006).
12. B. Kyung, S. S. Kancharla, D. Senechal, et al., Phys. Rev. B **73**, 165114 (2006).
13. S. Sakai, Y. Motome, and M. Imada, Phys. Rev. Lett. **102**, 056404 (2009).
14. A. Liebsch and N.-H. Tong, Phys. Rev. B **80**, 165126 (2009).
15. M. Civelli, Phys. Rev. B **79**, 195113 (2009).
16. M. Potthoff, Eur. Phys. J. B **32**, 429 (2003).
17. T. Maier, M. Jarrell, T. Pruschke, and M. Hettler, Rev. Mod. Phys. **77**, 1027 (2005).
18. G. Kotliar, S. Y. Savrasov, K. Haule, et al., Rev. Mod. Phys. **78**, 865 (2006).
19. D. Senechal, D. Perez, and M. Pioro-Ladriere, Phys. Rev. Lett. **84**, 522 (2000).
20. R. O. Zaitzev, J. Exp. Theor. Phys. **43**, 574 (1976).
21. A. A. Kordyuk, S. V. Borisenko, M. Knupfer, and J. Fink, Phys. Rev. B **67**, 064504 (2003).
22. W. Prestel, F. Venturini, B. Muschler, et al., Eur. Phys. J. ST **188**, 163 (2010).
23. T. Yoshida, X. J. Zhou, D. H. Lu, et al., Condens. Matter **19**, 125209 (2007).
24. D. S. Marshall, D. S. Dessau, A. G. Loeser, et al., Phys. Rev. Lett. **76**, 4841 (1996).
25. A. Ino, C. Kim, M. Nakamura, et al., Phys. Rev. B **62**, 4137 (2000).
26. T. Yoshida, M. Hashimoto, T. Takizawa, et al., Phys. Rev. B **82**, 085119 (2010).
27. K. Ishizaka, T. Kiss, S. Izumi, et al., Phys. Rev. B **77**, 064522 (2008).